Contents lists available at ScienceDirect

Biochemistry and Biophysics Reports

A simple indirect colorimetric assay for measuring mitochondrial energy metabolism based on uncoupling sensitivity

Patries M. Herst [a,b,*], Carole Grasso [a], Marie-Sophie Fabre [a,c], Stepana Boukalova [a,d], Zuzana Ezrova [d,e], Jiri Neuzil [d], Michael V. Berridge [a]

[a] Malaghan Institute of Medical Research, PO Box 7060, Wellington, New Zealand
[b] Department of Radiation Therapy, University of Otago, Wellington, New Zealand
[c] School of Biological Sciences, University of Victoria, Wellington, New Zealand
[d] Institute of Biotechnology, Czech Academy of Sciences, 25250, Prague-West, Czech Republic
[e] Faculty of Science, Charles University, 128 44, Prague, Czech Republic

ARTICLE INFO

ABSTRACT

Purpose: Cancer cells rapidly adjust their balance between glycolytic and mitochondrial ATP production in response to changes in their microenvironment and to treatments like radiation and chemotherapy. Reliable, simple, high throughput assays that measure the levels of mitochondrial energy metabolism in cells are useful determinants of treatment effects. Mitochondrial metabolism is routinely determined by measuring the rate of oxygen consumption (OCR). We have previously shown that indirect inhibition of plasma membrane electron transport (PMET) by the mitochondrial uncoupler, FCCP, may also be a reliable measure of mitochondrial energy metabolism. Here, we aimed to validate these earlier findings by exploring the relationship between stimulation of oxygen consumption by FCCP and inhibition of PMET.

Methods: We measured PMET by reduction of the cell impermeable tetrazolium salt WST-1/PMS. We characterised the effect of different growth conditions on the extent of PMET inhibition by FCCP. Next, we compared FCCP-mediated PMET inhibition with FCCP-mediated stimulation of OCR using the Seahorse XF96e flux analyser, in a panel of cancer cell lines.

Results: We found a strong inverse correlation between stimulation of OCR and PMET inhibition by FCCP. PMET and OCR were much more severely affected by FCCP in cells that rely on mitochondrial energy production than in cells with a more glycolytic phenotype.

Conclusion: Indirect inhibition of PMET by FCCP is a reliable, simple and inexpensive high throughput assay to determine the level of mitochondrial energy metabolism in cancer cells.

1. Introduction

The ability to rapidly adjust the balance between glycolytic and mitochondrial ATP production is a hallmark of highly aggressive, invasive and metastatic cancers. Bioenergetic plasticity, orchestrated through mitochondrial-to-nuclear crosstalk [1], confers a strong survival advantage in the tumour microenvironment that contains fluctuating oxygen and nutrient levels [2]. Under aerobic conditions, many tumour cells favour glycolysis in the presence of oxygen, also referred to as *the Warburg effect* [3–5]. Because oxidative phosphorylation (OXPHOS) is much more efficient at producing ATP per glucose consumed than glycolysis [6], tumour cells can maintain relatively low

OXPHOS rates (6% of maximum) and still obtain 50% of their energy requirements through this pathway [7]. Traditionally, the levels of mitochondrial energy production have been measured as oxygen consumption by an oxygen electrode and more recently by the Seahorse XF96e flux analyser. Here, we describe a quick, simple and reliable colorimetric assay that measures the level of plasma membrane electron transport (PMET) and can be easily adjusted to measure the level of mitochondrial energy metabolism. This assay could be a useful additional tool, particularly in the context of chemo- and radiation therapy resistance, which are often accompanied by shifts in energy metabolism.

Several plasma membrane electron transport (PMET) systems have been reported for mammalian cells, with different functions including

---

* Corresponding author. laghan Institute of Medical Research, PO Box 7060, Wellington, New Zealand.
  E-mail address: pherst@malaghan.org.nz (P.M. Herst).

cellular defence against pathogens, iron uptake, cell growth, intracellular redox status and cell signalling (reviewed in Ref. [8]). Our group has described in detail a PMET system that consists of an inward-facing NADH-oxidoreductase, CoQ and an outward-facing surface oxidase. This PMET activity can be measured colorimetrically by reduction of the cell impermeant tetrazolium dye, 2- (4-iodophenyl) -3- (4-nitrophenyl) -5-(2,4-disulfophenyl)-2H-tetrazolium monosodium salt (WST-1) into its highly coloured formazan, WST-1H, in the presence of its obligate intermediate electron acceptor, 1-methoxy-5-methyl phenazinium methylsulphate (PMS) (see Fig. 1 and [9]). WST-1/PMS reduction occurs extracellularly and is extensively inhibited by superoxide dismutase at the cell surface, the flavin centre inhibitor, diphenyleneiodonium, the NQ01 inhibitor, dicoumarol and the ubiquinone redox recycling inhibitors, capsaicin and resiniferatoxin [9,10]. Electrons from intracellular NADH travel through this short electron transfer chain in the plasma membrane to extracellular substrates at the cell surface. We showed that oxygen and PMS compete with each other at the cell surface for electrons coming through the electron chain. Strong WST-1/PMS activity is particularly evident in purely glycolytic cancer cells that are devoid of mitochondrial (mt)DNA (ρ^0 cells). These cells are unable to perform OXPHOS and are completely reliant on glycolytic ATP production. Highly glycolytic cells maintain a favourable NAD$^+$/NADH ratio through strong lactate dehydrogenase activity and PMET [9–11]. Many different types of cancer strongly reduce WST-1/PMS, particularly under hypoxic conditions [9].

In this manuscript we will refer to WST-1/PMS reduction as a measure of PMET activity simply as dye reduction. Reducing equivalents are produced in both the cytoplasm and the mitochondrial matrix and shuttle between both compartments through, for instance, the malate-aspartate shuttle. In this way, NADH generated during glycolysis can be recycled through mitochondrial electron transport (MET) and under hypoxic conditions, mitochondrially-generated NADH can be recycled through increased LDH and PMET activity (Fig. 1).

We previously measured oxygen consumption, using a Clark oxygen electrode, in a panel of 19 murine and human cancer cell lines. Total oxygen consumption was divided into mitochondrial oxygen consumption (inhibited by the respiratory complex III-inhibitor, myxothiazol), cell surface oxygen consumption (inhibited by extracellularly applied NADH) and basal oxygen consumption (not inhibited by either myxothiazol or NADH). Basal oxygen consumption is caused by the action of a number of oxygen consuming enzymes that are not part of the OXPHOS and PMET systems, such as the monoamine oxidases, the prolyl hydroxylase domain enzymes, the cyclo-oxygenases and many peroxisomal enzymes. Basal oxygen consumption rates vary between different cell types but is never affected by FCCP. Cell surface oxygen consumption, but not mitochondrial oxygen consumption or basal oxygen consumption, correlated closely with dye reduction, with very similar inhibitor profiles [9]. In the presence of the protonophore, FCCP, the inner mitochondrial membrane becomes permeable to protons, abolishing the mitochondrial membrane potential, an absolute requirement for OXPHOS [12]. In response to FCCP, cells rapidly increase mitochondrial oxygen consumption in an attempt to rebuild the mitochondrial membrane potential. This depletes cellular NADH levels, resulting in decreased dye reduction and cell surface oxygen consumption (Fig. 1).

In this paper, we revisit FCCP-mediated inhibition of dye reduction in more detail using the metastatic murine breast cancer 4T1 and 4T1 ρ^0 cells and different conditions that affect the level of mitochondrial
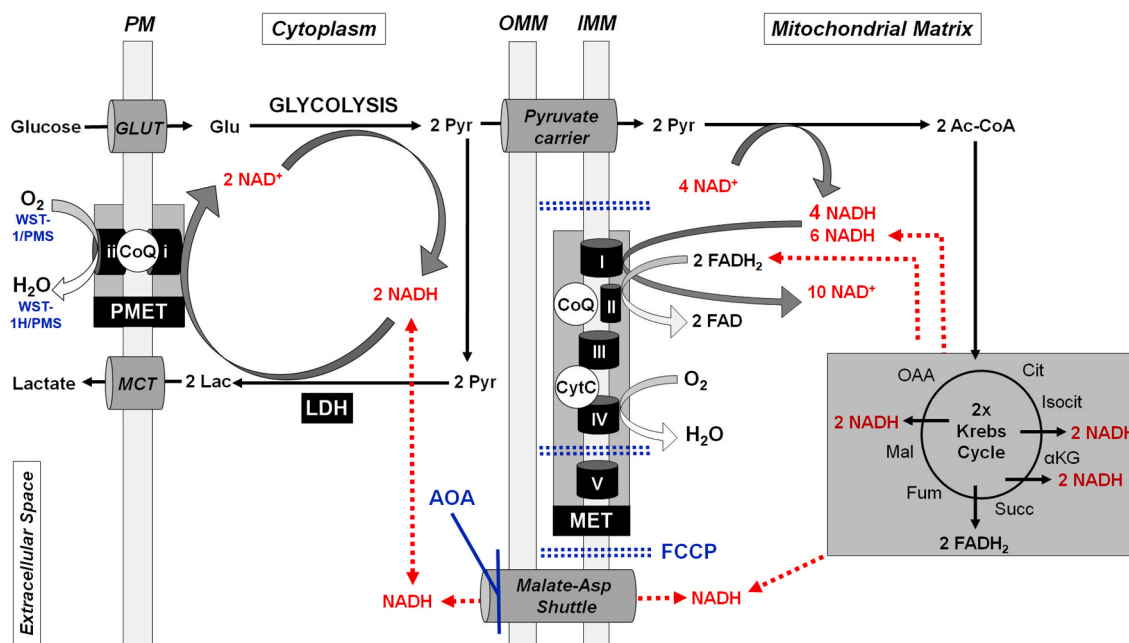

Fig. 1. **Diagram of cellular energy production and NADH recycling.** NADH is produced during glycolysis, oxidation of pyruvate to acetyl-CoA and during the Krebs cycle. Under optimal conditions, mitochondrial NADH production accounts for 80% of total NADH production (10NADH/glucose). Re-oxidation of NADH occurs during mitochondrial electron transport (MET), plasma membrane electron transport (PMET) and through the activity of lactate dehydrogenase (LDH). MET consists of 4 respiratory complexes, CoQ and CytC. PMET consists of an inward-facing NADH-oxidoreductase (i), CoQ and an outward-facing surface oxidase (ii) and can be measured by reduction of the water-soluble cell-impermeant tetrazolium salt, WST-1 in the presence of its obligate intermediate electron acceptor, PMS. The malate-aspartate shuttle transports reducing equivalents between the cytoplasm and the mitochondrial matrix in both directions and is inhibited by aminooxyacetate (AOA). The protonophore, FCCP, increases mitochondrial oxygen consumption to maintain the mitochoindrial membrane potential. This increases mitochondrial NADH recycling and decreases the amount of NADH available for recycling by PMET and LDH. *Ac-CoA: acetyl-CoA, AOA: aminooxyacetate, Cit: citrate, CytC: cytochrome C, CoQ: coenzyme Q10, FCCP: carbonyl cyanide-4-(trifluoromethoxy)phenylhydrazone, Fum: fumarate, Glu: glucose, GLUT: glucose transporter, IMM: inner mitochondrial membrane, Isocit: isocitrate, αKG: α-ketoglutarate, Lac: lactate, LDH: lactate dehydrogenase, Mal: malate, MCT: monocarboxylate transporter, MET: mitochondrial electron transport, OMM: outer mitochondrial membrane, OAA: oxaloacetate, PM: plasma membrane, PMET: plasma membrane electron transport, PMS: 1-methoxy-5-methyl phenazinium methylsulphate, Pyr: pyruvate, Succ: succinate, WST-1: 2- (4-iodophenyl) -3- (4-nitrophenyl) -5- (2,4-disulfophenyl) -2H- tetrazolium monosodium salt.*

metabolism. In addition, we compare the extent of FCCP-mediated inhibition of dye reduction with the extent of FCCP-mediated stimulation of mitochondrial oxygen consumption, using the Seahorse XF96e flux analyser, in a number of different cancer cell lines.

2. Materials and methods

2.1. Cell lines and cell culture techniques

The GBM cell line, LN18, and the metastatic triple negative cell line, 4T1, were obtained from the American Type Culture Collection; the human pancreatic cancer cell line, PaTu8902, was obtained from the German Collection of Microorganisms and Cell Cultures GmbH (Leipniz Institute); the mouse glioma cell line, GL261 was obtained from the NCI tumour-cell-line repository (Frederick, MD, USA); the murine mastocytoma cell line P815 was a kind gift from Dr. John. Marbrook (University of Auckland, NZ). All mammalian cell lines were grown in RPMI-1640 medium or DMEM medium supplemented with 10% (v/v) fetal bovine serum, GlutaMAX-1 (2 mM), penicillin (100 U/mL) and streptomycin sulfate (100 μg/mL). Media was supplemented with uridine (50 μg/μL) and pyruvate (1 mM) for all ρ^0 cells which were derived from their parental strains by long-term culture (6–12 weeks) with 50 ng/mL filter-sterilized ethidium bromide (EtBr) according to the protocol of King and Attardi [13]. The ρ^0 status of all ρ^0 cell lines was verified by PCR to confirm the absence of mtDNA. Cells were maintained at 37 °C and 5% CO_2 in a humidified incubator.

3. Materials

Unless otherwise noted, tissue plasticware was purchased from Nunc (ThermoFisher Scientific, Auckland, New Zealand); all cell culture reagents were from Gibco BRL (Invitrogen, Auckland, New Zealand). WST-1 (2-(4-iodophenyl) -3- (4-nitrophenyl) -5- (2,4-disulfophenyl) -2H-tetrazolium mono sodium salt) and PMS (1-methoxy- phenazine methosulfate) were purchased from Dojindo Laboratories (Kumamoto, Japan). Unless otherwise stated all other reagents were from Sigma Chemical Company (St. Louis, MO., U.S.A.).

3.1. WST-1/PMS reduction

WST-1/PMS reduction rates were measured in a microplate format as described previously [9]. Briefly, exponentially growing cells were centrifuged at $130 \times g$ for 5 min, washed and resuspended in HBSS buffer. For each assay, unless specified differently, 50 μL of a 2×10^6 cells/mL cell suspension was pipetted into microplate wells containing 50 μL of the inhibitor/buffer solution (10 μL of the 10x stock solution added to 40 μL of HBSS buffer), resulting in a final concentration of 1×10^6 cells/mL. Dye reduction was initiated by adding 10 μL of a 10x stock solution of WST-1/PMS in milliQ water (final concentrations of 500 μM WST-1 and 20 μM PMS). WST-1 reduction was measured in real time at 450 nM over 30–60 min in a Tecan plate reader. Inhibition of WST-1/PMS reduction by FCCP was determined by measuring WST-1/PMS reduction in the presence and absence of 2 μM FCCP, unless stated differently. Percentage control was calculated as (A450/min with FCCP divided by A450/min without FCCP)x100. Percentage FCCP inhibition was calculated as 100-% control.

3.2. Radiation treatment of GL261

Cells were seeded approximately 24h before treatment at $2–4 \times 10^5$ cells in T25 tissue culture flasks. Cells were approximately 30% confluent and growing exponentially on the day of treatment. Cells were irradiated using Cesium-137 γ-rays (Gammacell 3000 Elan) with 3 Gy (GL261 3Gy). After irradiation cells were cultured for xxx.

3.3. Temozolomide treatment of GL261

A GL261 cell line resistant to Temozolomide (GL261_TMZ-R) was generated by treating GL261 with increasing concentration of TMZ (10, 30, 50, 100, 150, 200, 400 μM). Cells were treated for 72 h with each concentration and maintained in culture in TMZ 80 μM. The resistant phenotype was confirmed by a clonogenic assay, showing that GL261 TMZR was able to form colonies after a single treatment with 400 μM TMZ, whilst GL261 did not form any colonies after a single exposure to 400 μM TMZ.

3.4. Generation of PaTu cell lines

The human pancreatic cancer cell line PaTu 8902 with inactivated SMAD4 (PaTu8902_SMAD4_KO), an important mediator of transforming growth factor β pathway, was created by CRISPR/Cas9 technology. Reconstitution of SMAD4 was performed by lentiviral transduction of SMAD4 KO cells with *hSMAD4*-containing vector.

3.5. Oxygen consumption rates as measured by seahorse

The Seahorse XF96e extracellular flux analyser (Bioscience) was used to measure cellular oxygen consumption rate (OCR) as per manufacturer's instructions. Briefly, cells were seeded into Seahorse XF96 cell culture microplates pre-coated with Cell-Tak solution (Corning) 10,000–50,000 per plate, depending on cell type, the day before the experiment. After 24 h, the medium was replaced with Seahorse XF base medium supplemented with 5 mM HEPES, 10 mM glucose and 1 mM pyruvate with pH adjusted to 7.4, and the microplates were placed in non-CO_2 incubator for 60 min. The assay protocol consisted of four consecutive injection steps in which 1 μM oligomycin, 2 μM FCCP and the combination of 0.5 μM Rotenone and 0.5 μM Antimycin A were added. Lastly, Hoechst 33342 was injected in concentration 5 μg/mL in order to assess the number of cells present in each well. The data were normalized to intensity of Hoechst staining determined by Tecan plate reader absorption at A490.

4. Results

4.1. Dye reduction is fuelled predominantly by mitochondrial reducing equivalents

Aminooxyacetate (AOA) is an inhibitor of the malate-aspartate shuttle [14–16] that reversibly tranfers NADH reducing equivalents across the mitochondrial membrane. The effect of different concentrations of AOA on dye reduction in 4T1 cells is shown in Fig. 2A, with 2 mM AOA inhibiting dye reduction by $76 \pm 3\%$. Higher concentrations of AOA did not completely inhibit dye reduction, indicating that although the vast majority of NADH that fuels dye reduction originates in the mitochondria, glycolytically produced NADH may also play a small role.

4.2. FCCP inhibits dye reduction

FCCP is used as an uncoupler of MET and OXPHOS [12] in assays that measure OCR, such as the Oxygraph and the Seahorse XF analyser, at concentrations between 1 and 3 μM [17]. We determined the effect of different FCCP concentrations on dye reduction with different numbers of 4T1 cells (Figs. 2B) and 4T1ρ^0 cells (Fig. 2C). FCCP decreased dye reduction in 4T1 cells in a dose-dependent manner, but did not affect dye reduction in 4T1ρ^0 cells. Fig. 2D and E show representative primary data for WST-1/PMS reduction for 4T1 and 4T1ρ^0 cells respectively.

Next, we determined how different culture conditions affected the extent of FCCP-mediated inhibition of dye reduction in 4T1 cells (Fig. 3). Switching from RPMI (2 g/L glucose, no pyruvate) to DMEM (4.5 g/L glucose, no pyruvate) (Fig. 3A) did not alter the FCCP effect. However, the addition of 1 mM pyruvate to RPMI medium (Fig. 3B) decreased the
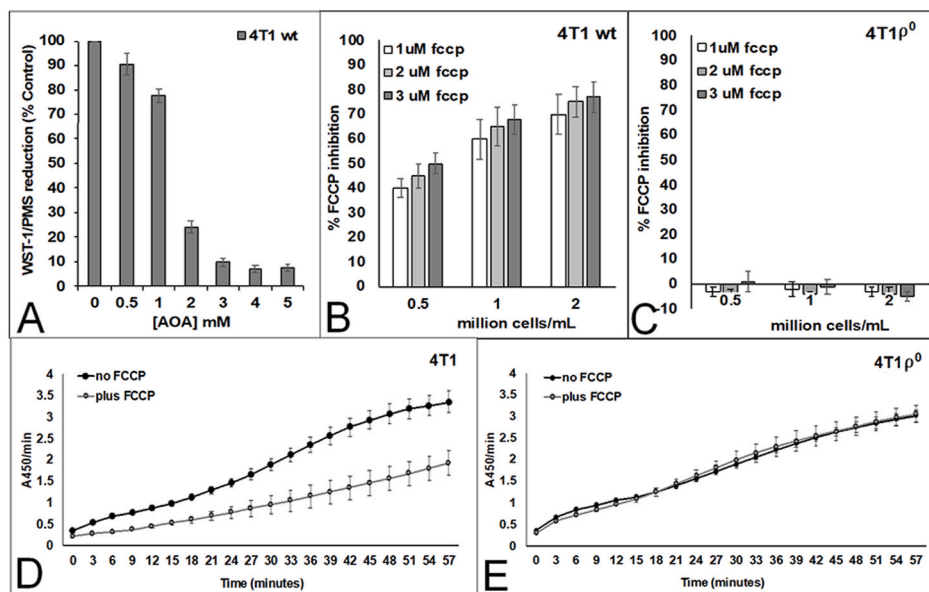
Fig. 2. The effect of AOA (A) and different concentration of FCCP on dye reduction by 4T1 cells (B) and 4T1ρ^0 cells (C). A] 4T1 cells (10^6/mL) were exposed to different concentrations of the malate/aspartate shuttle inhibitor, AOA, for 10 min and dye reduction was measured as milliA450/min. Values of treated cells are normalized to those of untreated control cells. B] Different concentrations of 4T1 cells and C] 4T1 ρ^0 cells were exposed to 0, 1, 2 and 3 μM FCCP for 10 min. The % FCCP inhibition was calculated as 100-(A450/min with FCCP divided by A450/min without FCCPx100). Experiments were done at least three times in triplicate. Raw data for one experiment with 1×10^6 4T1 cells, showing a 60% inhibition of dye reduction by FCCP measured at the linear part of the curve (D) and no effect of FCCP on dye reduction in 0.5×10^6 4T1ρ^0 cells (E).
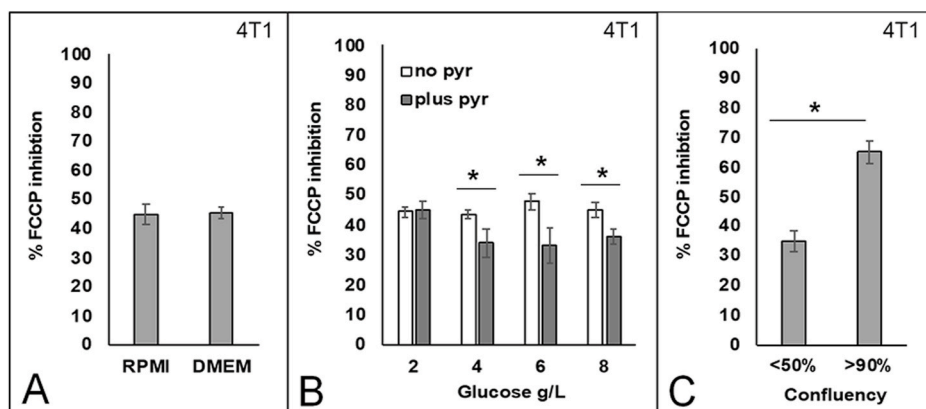

Fig. 3. The effect of type of medium (A), glucose and pyruvate (B) and confluency (C) on inhibition of dye reduction by 2 μM FCCP in 4T1 cells. 4T1 Cells were incubated under the conditions specified for 24–48h. Unless stated differently, cells were harvested at 40–60% confluency. The % FCCP inhibition was calculated as 100-(A450/min with FCCP divided by A450/min without FCCPx100). Experiments were carried out three times in triplicate. *: p < 0.05.

inhibition of dye reduction by FCCP by approximately 25%, which was independent of the glucose concentration. The effect of FCCP on dye reduction was also lower in actively growing cells compared to confluent cells (Fig. 3C).

4.3. The effects of FCCP on dye reduction and oxygen consumption are strongly inversely correlated

We measured inhibition of dye reduction and stimulation of OCR by FCCP (also referred to as the Reserve Respiratory Capacity) in a number of different cancer cell lines, using the Seahorse XF96e analyser (Fig. 4). An annotated representative oxygen consumption profile is presented in Fig. 4A. Representative oxygen consumption profiles for 4T1 and 4T1ρ^0 cells are depicted in Fig. 4B. The Table in Fig. 4C lists the cell types used and their values for % inhibition of dye reduction and OCR stimulation by FCCP. We found that stimulation of OCR by FCCP was strongly inversely correlated with inhibition of dye reduction (Fig. 4C and D). In GL261 cells, the effect of FCCP on both dye reduction and OCR was lowest in ρ^0 cells and highest in temozolomide resistant GL261 cells (GL261 TMZR). Similarly, the effect of FCCP on dye reduction and OCR was lower in PaTu 8902 human ductal pancreatic adenocarcinoma cells with their *SMAD4* gene deleted (PaTu8902_SMAD4_KO) compared with

their parental counterparts and PaTu 8902_SMAD4_KO cells with the *SMAD4* gene inserted (PaTu8902_SMAD4_rec; Ezrova et al. manuscript submitted).

5. Discussion

Most cancer cells are able to continuously adjust the contributions of glycolytic and mitochondrial ATP production to respond to changes in their microenvironment, such as those caused by chemo- and radiation therapy [7]. A quick, simple and reliable initial screening assay to measure the contribution of OXPHOS to energy metabolism would be a useful additional tool, particularly in high throughput systems. Our assay consists of a simple 96 well tetrazolium dye reduction (WST-1/PMS) system. The extent of mitochondrial energy production is represented by the level of inhibition of dye reduction by ionophore FCCP. In this manuscript we show that the effects of FCCP on dye reduction and mitochondrial oxygen consumption are strongly inversely correlated ($R^2 = 0.98$), using the Seahorse XF96 extracellular flux analyser. Changes in the extent of FCCP-mediated inhibition of dye reduction gave a rapid indication of the effectiveness of treatments that induce a glycolytic shift. For instance, radiation therapy has been shown to make cancer cells more glycolytic by increasing the level of reactive
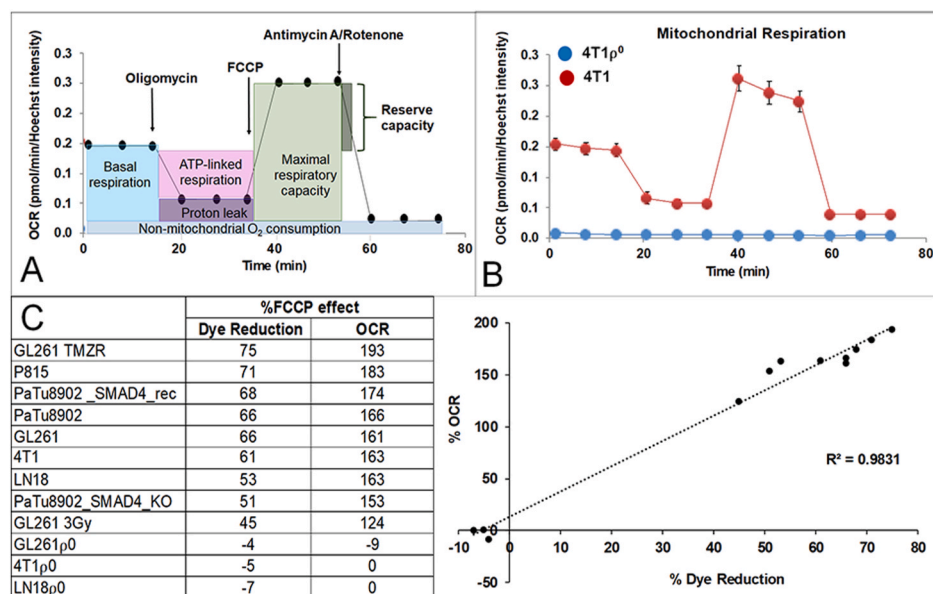
Fig. 4. The effect of 2 μM FCCP on dye reduction and OCR in different cancer cell lines. A] Seahorse XFe analysis of oxygen consumption profiles after oligomycin (complex V inhibitor), FCCP (protonophore) and Antimycin A (complex III inhibitor)/Rotenone (complex I inhibitor). B] oxygen consumption profiles of 4T1 and 4T1 ρ^0 cells. Dye reduction was measured as A450/min and OCR was measured using the Seahorse XF96e flux analyser. C] Table shows % inhibition of dye reduction and % OCR stimulation by FCCP for various cancer cell lines: GL261 (murine glioblastoma), P815 (murine mastocytoma), PaTu8902 (human pancreatic cancer), 4T1 (murine metastatic breast cancer), LN18 (human glioblastoma). GL261 and LN18 cells were grown in DMEM; the other cell lines were grown in RPMI. The graph shows a strong inverse correlation between the effect of FCCP on OCR and dye reduction ($R^2 = 0.9831$). FCCP experiments were carried out at least 3 times in triplicate; OCR experiments were carried out at least 2 times in triplicate.

oxygen species and stabilising HIF-1α [18–20]. Our results support such a glycolytic shift as evidenced by a smaller FCCP effect in murine glioma GL261 cells exposed to a single dose of 3Gy compared with unexposed cells. In addition, decreasing the level of mitochondrial metabolism by knocking out *SMAD4* from human pancreatic PaTu8902 cells also decreased the FCCP effect, which was restored to parental levels after the *SMAD4* gene was reconstituted. SMAD4 is an important mediator of the transforming growth factor β pathway. PaTu8902_SMAD4_KO cells have been shown to have a lower level of mitochondrial metabolism compared with their parental cells (Ezrova et al. manuscript submitted). In contrast, the FCCP effect was stronger in GL261 cells resistant to 400 μM temozolomide. Remodelling of mitochondrial electron transport as a result of temozolomide resistance, resulting in increased mitochondrial respiratory capacity has been described in temozolomide-resistant human GBM U251 cells [21].

PMET, measured as WST-1/PMS dye reduction, is highly active in glycolytic cells [9]. Here, we show that mitochondrially generated NADH is a major contributor to dye reduction at the cell surface, as evidenced by a 80% recrease in dye reduction in the presence of 2 mM AOA, a malate-aspartate inhibitor [14–16]. FCCP inhibits dye reduction at the cell surface by removing available reducing equivalents through an increase in OCR (Fig. 1). We show that growth conditions that affect the level of mitochondrial metabolism also affect the extent of FCCP-mediated inhibition of dye reduction. As expected, FCCP had no effect in purely glycolytic ρ^0 cells that are incapable of OXPHOS. Most rapidly proliferating cancer cells strongly depend on glycolysis even in the presence of oxygen ("Warburg effect") for their energy requirements. These cells use glucose, nucleotides, amino acids, and lipids as anabolic resources to create more biomass, in preference to generating ATP more efficiently in pathways that generate CO_2 instead of biomass. Contact-inhibited confluent cells proliferate more slowly, if at all and thus have lower anabolic needs than rapidly proliferating cells. Therefore, confluent cells rely more on mitochondrial OXPHOS for ATP production [4,5]. The higher glycolytic activity of actively growing 4T1 cells in our assays was mirrored by a smaller FCCP effect compared with confluent 4T1 cells. Adding extracellular pyruvate saturates pyruvate dehydrogenase activity, leaving excess pyruvate to generate lactate and cytoplasmic NAD^+ [4], which decreases the cell's reliance on mitochondrial electron transport to generate NAD^+ and thus decreases the FCCP effect. The fact that additional pyruvate decreased the FCCP effect on PMET could be relevant as dye reduction assays were done in HBSS without pyruvate and OCR experiments were done in RPMI with

pyruvate. Had all PMET assays been done in RPMI rather than HBSS, the FCCP effect would have been smaller in all instances and this would have flattened the correlation graph in Fig. 4D to some extent, but would have had little effect on the strength of the correlation itself.

We believe that PMET may be an evolutionary remnant of ancestral eukaryotes and will be found in the cell membrane of all cells, cancer and non-cancerous. We have previously found robust PMET activities in a panel of 19 human and murine cancer and non-cancer cell lines, several of whom had very strong OXPHOS activity [9]. We have also shown strong PMET activities in primary immune cells, WI38 fibroblasts and HUVECs [22]. However, it is important to note that this assay is limited to dilute cell suspensions and to metaboliocally active cells. We did successfully use FCCP-inhibition of PMET on bone marrow samples of leukemic patients and demonstrated that patients with highly glycolytic blasts had a better prognosis [23]. Tissues other than blood, lymph and bone marrow would need to be macerated and treated with enzymes that digest the extracellular matrix, cell to cell junctions etc. to produce cell suspensions and this could affect metabolic activity. This is unfortunately a limitation of many advanced analytical techniques such as the Seahorse Extracellular flux analyser and techniques using flow cytometry.

Another limitation of this dye reduction assay is that it uses FCCP as a mitochondrial uncoupler which has off-target effects such as plasma membrane depolarisation, which is potentially an issue with an assay that requires an intact plasma membrane and metabolically active cells. Low concentrations (1–2 μM) of FCCP were found not to be toxic and only transiently decreased the plasma membrane potential in L6 myoblasts, whilst higher concentrations (10 μM) of FCCP decreased the plasma membrane potential substantially [24]. In our hands, 2 μM FCCP has not shown any toxicity with the cell lines and primary cells we have used, but if FCCP toxicity is of concern, other mitochondrial uncouplers that do not have these off-target effects may be an option [24].

In conclusion, we contend that the extent of FCCP-mediated inhibition of reduction of the cell-impermeant tetrazolium dye, WST-1/PMS, is a reliable, fast and easy assay to measure the level of mitochondrial energy metabolism. We envisage that the assay described here will be used as an initial screening assay to quickly assess leves of mitochondrial metabolism. However, results of this assay need to be validated by oxygen consumption measurements using oxygen electrodes such as the Oxygraph, or platforms such as the Seahorse Extracellular flux analyser.

Declaration of competing interest

The authors declare that they have no known competing financial interests or personal relationships that could have appeared to influence the work reported in this paper.

Acknowledgements

References

[1] T. Arnould, S. Michel, P. Renard, Mitochondria retrograde signaling and the UPR mt: where are we in mammals? Int. J. Mol. Sci. 16 (2015) 18224–18251, https://doi.org/10.3390/ijms160818224.

[2] P. Herst, M. Rowe, G. Carson, M. Berridge, Functional mitochondria in health and disease, Front. Endocrinol. 8 (2017) e296, https://doi.org/10.3389/fendo.2017.00296.

[3] O. Warburg, On the origin of cancer ells, Nature 123 (1956) 309–314.

[4] J.S. Burns, G. Manda, Metabolic pathways of thewarburg effect in health and disease: perspectives of choice, chain or chance, Int. J. Mol. Sci. 18 (2017) 1–28, https://doi.org/10.3390/ijms18122755.

[5] M.G. VanderHeiden, L.C. Cantley, C.B. Thompson, Understanding the Warburg effect: the metabolic requirementsof cell proliferation, Science 84 324 (2009) 1029–1033, https://doi.org/10.1126/science.1160809.Understanding.

[6] S.A. Mookerjee, A.A. Gerencser, D.G. Nicholls, M.D. Brand, Quantifying intracellular rates of glycolytic and oxidative ATP production and consumption using extracellular flux measurements, J. Biol. Chem. 292 (2017) 7189–7207, https://doi.org/10.1074/jbc.M116.774471.

[7] P.M. Herst, C. Grasso, M.V. Berridge, Metabolic reprogramming of mitochondrial respiration in metastatic cancer, Canc. Metastasis Rev. 37 (2018) 643–653, https://doi.org/10.1007/s10555-018-9769-2.

[8] J.D. Ly, A. Lawen, Transplasma membrane electron transport: enzymes involved and biological function, Redox Rep. 8 (2003) 3–21, https://doi.org/10.1179/135100003125001198.

[9] P.M. Herst, M.V. Berridge, Cell surface oxygen consumption: a major contributor to cellular oxygen consumption in glycolytic cancer cell lines, Biochim. Biophys. Acta Bioenerg. 1767 (2007) 170–177, https://doi.org/10.1016/j.bbabio.2006.11.018.

[10] P. Herst, A. Tan, D.-J. Scarlett, M. Berridge, Cell surface oxygen consumption by mitochondrial gene knockout cells, Biochim. Biophys. Acta 1656 (2004) 79–87, https://doi.org/10.1016/j.bbabio.2004.01.008.

[11] P. Herst, M. Berridge, Plasma membrane electron transport: a new target for cancer drug development, Curr. Mol. Med. 6 (2006) 895–904.

[12] Demine, Arnould Renard, Mitochondrial Uncoupling, A key controller of biological processes in physiology and diseases, Cells 8 (2019) 795, https://doi.org/10.3390/cells8080795.

[13] M.P. King, G. Attardi, Human cells lacking mtDNA: repopulation with exogenous mitochondria by complementation, Science 246 (1989) 500–503, https://doi.org/10.1126/science.2814477.

[14] M. Mitchell, K.S. Cashman, D.K. Gardner, J.G. Thompson, M. Lane, Disruption of mitochondrial malate-aspartate shuttle activity in mouse blastocysts impairs viability and fetal Growth1, Biol. Reprod. 80 (2009) 295–301, https://doi.org/10.1095/biolreprod.108.069864.

[15] N.B. Støttrup, B. Løfgren, R.D. Birkler, J.M. Nielsen, L. Wang, C.A. Caldarone, S. B. Kristiansen, H. Contractor, M. Johannsen, H.E. Bøtker, T.T. Nielsen, Inhibition of the malate-aspartate shuttle by pre-ischaemic aminooxyacetate loading of the heart induces cardioprotection, Cardiovasc. Res. 88 (2010) 257–266, https://doi.org/10.1093/cvr/cvq205.

[16] N.R. Jespersen, T. Yokota, N.B. Støttrup, A. Bergdahl, K.B. Pælestik, J.A. Povlsen, F. Dela, H.E. Bøtker, Pre-ischaemic mitochondrial substrate constraint by inhibition of malate-aspartate shuttle preserves mitochondrial function after ischaemia–reperfusion, J. Physiol. 595 (2017) 3765–3780, https://doi.org/10.1113/JP273408.

[17] M. Wu, A. Neilson, A.L. Swift, R. Moran, J. Tamagnine, D. Parslow, S. Armistead, K. Lemire, J. Orrell, J. Teich, S. Chomicz, D.A. Ferrick, Multiparameter metabolic analysis reveals a close link between attenuated mitochondrial bioenergetic function and enhanced glycolysis dependency in human tumor cells, Am. J. Physiol. Cell Physiol. 292 (2007) 125–136, https://doi.org/10.1152/ajpcell.00247.2006.

[18] J. Zhong, N. Rajaram, D. Brizel, A. Frees, N. Ramanujam, I. Batinic-Haberle, M. Dewhirst, Radiation induces aerobic glycolysis through reactive oxygen species, Radiother. Oncol. 106 (2013) 390–396, https://doi.org/10.1016/j.radonc.2013.02.013.

[19] B.J. Moeller, Y. Cao, C.Y. Li, M.W. Dewhirst, Radiation activates HIF-1 to regulate vascular radiosensitivity in tumors: role of reoxygenation, free radicals, and stress granules, Canc. Cell 5 (2004) 429–441, https://doi.org/10.1016/S1535-6108(04)00115-1.

[20] W. Zhou, D.R. Wahl, Metabolic abnormalities in glioblastoma and metabolic strategies to overcome treatment resistance, Cancers 11 (2019) 1231, https://doi.org/10.3390/cancers11091231.

[21] C.R. Oliva, S.E. Nozell, A. Diers, S.G. McClugage, J.N. Sarkaria, J.M. Markert, V. M. Darley-Usmar, S.M. Bailey, G.Y. Gillespie, A. Landar, C.E. Griguer, Acquisition of temozolomide chemoresistance in gliomas leads to remodeling of mitochondrial electron transport chain, J. Biol. Chem. 285 (2010) 39759–39767, https://doi.org/10.1074/jbc.M110.147504.

[22] P. Herst, T. Petersen, P. Jerram, J. Baty, M. Berridge, The antiproliferative effects of phenoxodiol are associated with inhibition of plasma membrane electron transport in tumour cell lines and primary immune cells, Biochem. Pharmacol. 74 (2007) 1587–1595.

[23] P.M. Herst, R.A. Howman, P.J. Neeson, M.V. Berridge, D.S. Ritchie, The level of glycolytic metabolism in acute myeloid leukemia blasts at diagnosis is prognostic for clinical outcome, J. Leukoc. Biol. 89 (2011) 51–55, https://doi.org/10.1189/jlb.0710417.

[24] B.M. Kenwood, J.L. Weaver, A. Bajwa, I.K. Poon, F.L. Byrne, B.A. Murrow, J. A. Calderone, L. Huang, A.S. Divakaruni, J.L. Tomsig, K. Okabe, R.H. Lo, G. Cameron Coleman, L. Columbus, Z. Yan, J.J. Saucerman, J.S. Smith, J. W. Holmes, K.R. Lynch, K.S. Ravichandran, S. Uchiyama, W.L. Santos, G. W. Rogers, M.D. Okusa, D.A. Bayliss, K.L. Hoehn, Identification of a novel mitochondrial uncoupler that does not depolarize the plasma membrane, Mol. Metab. 3 (2014) 114–123, https://doi.org/10.1016/j.molmet.2013.11.005.